Journal of Thermal Analysis, Vol. 42 (1994) 781-791

DSC CALIBRATION IN THE STUDY OF SHAPE MEMORY ALLOYS

G. Airoldi[1], *G. Riva*[2], *B. Rivolta*[3] *and M. Vanelli*[1]

[1]Dip. Fisica, Università di Milano, via Celoria 16, 20133 Milano, Italy
[2]I.N.F.M., Unità di Milano Università, via Celoria 16, 20133 Milano, Italy
[3]Dip. Chimica Fisica Applicata, Politecnico di Milano, P.za L. daVinci 32, 20133 Milano, Italy

Abstract

The unusual mechanical properties (i.e. shape memory effect and superelasticity) of shape memory alloys (*SMA*) rely on the thermoelastic martensitic transformation (*TMT*) which is a first-order solid-solid, non-diffusive phase transition, athermal in character.

Differential scanning calorimetry (DSC) is often used as a convenient method of investigating the thermal properties of *SMAs*. The common practice of standard temperature calibration, required for a correct instrument performance, is here critically discussed in relation to the study of both the direct exothermic transformation on cooling, and the reverse endothermic transformation on heating in a NiTi *SMA*. The DSC results show that, with the standard temperature calibration, the instrument is calibrated on heating but un-calibrated on cooling. A general method is advanced to overcome this problem, intrinsically related to the dynamic character of DSC.

Keywords: DSC, shape memory alloys, temperature calibration

Introduction

Differential scanning calorimetry (DSC) is widely used as a convenient method of investigating the thermal properties of advanced materials [1, 2]. Characteristic temperatures and enthalpy changes associated with endothermic and exothermic processes are easily determined from the heat-flux *vs.* temperature curve [3].

In recent years, both theoretical [4] and experimental [5–7] papers devoted to the principles of DSC calibration, have been published. It has been pointed out that instrument calibration is critically related to experimental conditions such as scanning rate, sample pans, purge gas and so on. Moreover, instrument calibration by means of endothermic standards (e.g. melting of high purity metals such as In, Sn, Pb, Zn) is, in principle, strictly valid only for the study of endothermic transitions.

0368–4466/94/ $ 4.00

John Wiley & Sons, Limited
Chichester

Shape memory alloys exploit a reversible first order transition, the thermoelastic martensitic transformation (*TMT*), which is often investigated by DSC. The *TMT* transformation temperatures are relevant both in basic studies, to check the validity of theoretical models, and in applied research, to determine the operating temperatures of devices exploiting either the memory or superelastic effects. Moreover, in order to evaluate the transformation hysteresis, examination of both the direct exothermic *TMT* on cooling, and the reverse endothermic *TMT* on heating is required.

The standard DSC calibration, as usually performed exploiting two melting points of selected high purity metals, has been scrutinized in relation to the study of *TMT* in NiTi shape memory alloys, at the typical experimental scanning rates.

The standard temperature calibration

If T_s is defined as the actual sample temperature and T_{sm} the monitored sample temperature, the temperature calibration of a DSC aims to determine, as a function of T_{sm}, the temperature correction function $\Delta T(T_{sm}) = T_{sm} - T_s$. $\Delta T(T_{sm})$ depends upon two contributions: a dynamic and a static calibration factor.

The dynamic calibration factor

In the DSC, T_s differs from T_{sm}, due to its dynamical scanning character. Following [4], if R' is defined the thermal resistance between the sample pan and the temperature monitoring station, C_s the heat capacity of the specimen and $\dot{T}$ the scanning rate dT/dt, the dynamic temperature lag ΔT_{dyn} is:

$$\Delta T_{dyn}(\dot{T}) = T_{sm} - T_s = R' \times C_s \times \dot{T} = \tau_s \times \dot{T} \tag{1}$$

ΔT_{dyn} is a linear function of the scanning rate ($\dot{T}$), and is positive on heating for endothermic processes and negative on cooling for exothermic processes. Through the time-constant τ_s, ΔT_{dyn} depends upon both the sample (C_s) and the measuring conditions (R').

The static calibration factor

Usually, $T_{sm} \neq T_s$, even for $\dot{T} \to 0$. There is a static difference ΔT_{st}, which generally is a function of T_{sm}:

$$\Delta T_{st}(T_{sm}) = T_{sm} - T_s \quad (\dot{T} \to 0) \tag{2}$$

The temperature correction function is then:

$$\Delta T(T_{sm},\dot{T}) = \Delta T_{st}(T_{sm}) + \Delta T_{dyn}(\dot{T}) = \Delta T_{st}(T_{sm}) + \tau_s \times \dot{T} \quad (3)$$

In conclusion, $\Delta T\,(T_{sm},\ \dot{T})$ is a function of T_{sm}, a linear function of the scanning rate $\dot{T}$ with slope coefficient τ_s, and depends upon both the specific sample and measuring conditions. For a fixed $\dot{T}$, the two contributions cannot be separately obtained. However, using different scanning rates, the two contributions can be calculated by linear regression *vs.* $\dot{T}$.

In the standard two-point temperature calibration, $\Delta T\,(T_{sm},\ \dot{T})$ is evaluated, for a fixed $\dot{T}$, at the measured melting points (T_1 and T_2) of two calibration standards, and is linearly interpolated between T_1 and T_2. In other words:

$$\Delta T(T_{sm},\dot{T}) = \frac{\Delta T(T_2;\dot{T}) - \Delta T(T_1;\dot{T})}{T_2 - T_1} \times (T_{sm} - T_1) + \Delta T(T_1;\dot{T}) \quad (4)$$

Experimental procedure

DSC measurements were carried out by means of a Perkin Elmer DSC-7, provided with the Intracooler II cooling system. The calorimetric cell was purged by means of high purity (99.999%) nitrogen gas, at a flow rate of 20 cm^3/min. Special care was taken both to use low mass specimens and to put the specimens in the centre of standard 0219-0041 Al sample pans. High purity (99.999%) In (3.08 mg) and Pb (3.02 mg) Perkin Elmer calibration standards were used, with melting points of 156.60°C and 327.47°C, respectively. The standards were cut from a fresh surface.

The investigated SMA was a nearly equiatomic NiTi wire provided by the Furukawa El. Co. (Japan), drawn to a diameter of ø = 0.7 mm and aged at 500°C for 1.8 ks, under vacuum, followed by water quenching. The ageing treatment induces the presence of two *TMT*s. On cooling, the parent phase (*P*) with a b.c.c. lattice is transformed first into a rhombohedral phase (*R*), and at lower temperature, the R-phase is transformed into a monoclinic phase (*M*) [8, 9]. Attention was focused on the $P \leftrightarrow R$ TMT, known to have a high thermal stability under thermal cycling and a narrow hysteresis cycle (≈2°C) [10, 11]. Two specimens were investigated, A (6.53 mg) and B (12.99 mg).

The investigated DSC scanning rates were 0.1, 1, 10 and 20 deg·min^{-1}, both on cooling and on heating. With un-calibrated DSC, the scanning rates of 0.5, 5 and 50 deg·min^{-1} were also checked on the same NiTi specimens. For each scanning rate, the following procedure was adopted.

With un-calibrated DSC

a) All the calibration standards were melted three times before three DSC runs to evaluate the melting point (*m.p.*);

b) The $P \leftrightarrow R$ *TMT* was investigated, both on heating and on cooling, by two DSC runs;

c) The mean values of the melting point (<*m.p.*>) of In and Pb were used in the two-point temperature calibration of the DSC.

With calibrated DSC

d) same as a), in order to check the temperature calibration;

e) same as b).

Results

The measured values of <*m.p.*> of both In and Pb and the standard deviations (σ) obtained at the investigated $\dot{T}$, both with uncalibrated and calibrated

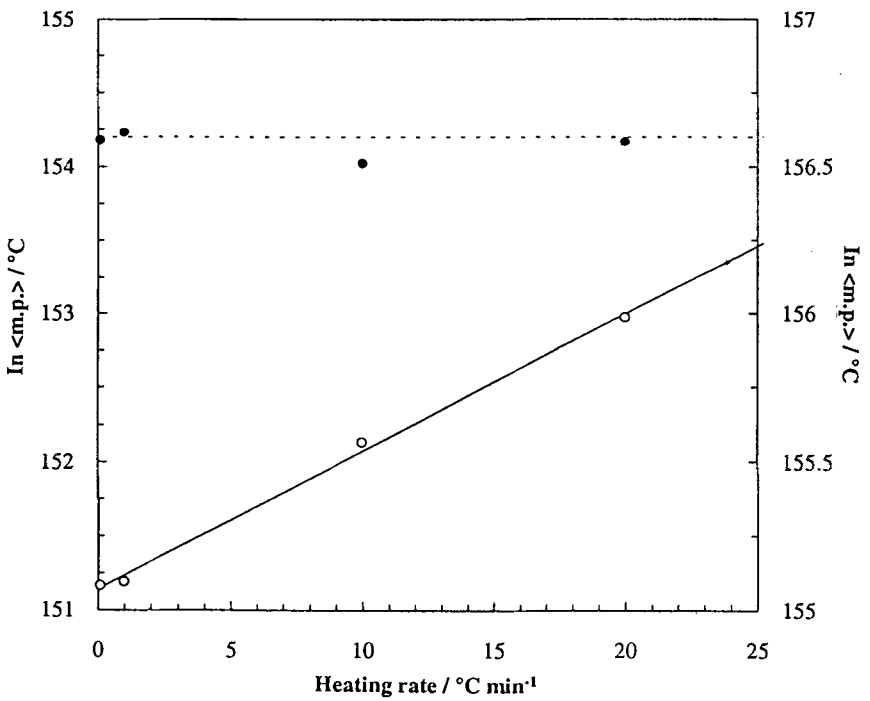

Fig. 1 Mean value of the In melting point (<*m.p.*>) as a function of the heating rate, with uncalibrated DSC (left axis, open symbols) and with calibrated DSC (right axis, full symbols): the regression line (—) and the reference In *m.p.* line (---) are also given

DSC, are reported in Tables 1 and 2, respectively. The NiTi $P \rightarrow R$ and $R \rightarrow P$ mean value onset temperatures ($<T_R>$ and $<T_R'>$, respectively) and the standard deviations, at the investigated $\dot{T}$ are also given in Tables 1 and 2. Table 3 reports, as calculated by a least square regression on the data in Table 1, the extrapolated $<m.p.>_{extr}$, $<T_R>_{extr}$ and $<T_R'>_{extr}$ for $\dot{T} \rightarrow 0$, with their respective standard deviations; the slope coefficient (τ) and the correlation factor (R). Similarly the data quoted in Table 4 are deduced from the results given in Table 2.

Table 1 $<m.p.>$ of In and Pb, $<T_R>$ and $<T_R'>$ of NiTi specimens (A and B) and their standard deviation (σ) at the investigated $\dot{T}$, obtained with uncalibrated DSC

	In		Pb	
$\dot{T}$ /	<m.p.>/	σ /	<m.p.>/	σ /
deg·min^{-1}		°C		
0.1	151.2	0.0	318.2	0.0
1	151.2	0.0	318.4	0.0
10	152.1	0.0	319.2	0.0
20	153.0	0.0	320.2	0.0
	NiTi (A) P→R		NiTi (B) P→R	
$\dot{T}$ /	T_R /	σ /	T_R /	σ /
deg·min^{-1}		°C		
0.1	35.6	0.1	35.5	0.1
0.5	35.5	0.0	35.6	0.0
1	35.6	0.0	35.5	0.0
5	35.1	0.0	35.0	0.0
10	34.5	0.0	34.4	0.0
20	33.3	0.0	33.2	0.0
50	29.4	0.0	29.1	0.0
	NiTi (A) R→P		NiTi (B) R→P	
$\dot{T}$ /	T_R' /	σ /	T_R' /	σ /
deg·min^{-1}		°C		
0.1	35.6	0.2	34.8	0.2
0.5	35.2	0.1	35.0	0.0
1	35.1	0.0	34.9	0.0
5	35.5	0.0	35.3	0.0
10	36.0	0.0	35.9	0.0
20	37.2	0.0	37.1	0.0
50	40.2	0.1	40.1	0.1

Table 2 <*m.p.*> of In and Pb, <T_R> and <T_R'> of NiTi specimens (A and B) and their standard deviation (σ) at the investigated $\dot{T}$, obtained with calibrated DSC

	In		Pb	
$\dot{T}$ /	<m.p.> /	σ /	<m.p.> /	σ /
deg·min^{-1}	°C			
0.1	156.6	0.0	327.4	0.0
1	156.6	0.0	327.5	0.0
10	156.5	0.0	327.5	0.0
20	156.6	0.0	327.4	0.1
	NiTi (A) P→R		NiTi (B) P→R	
$\dot{T}$ /	T_R /	σ /	T_R /	σ /
deg·min^{-1}	°C			
0.1	38.4	0.0	38.5	0.0
1	38.4	0.0	38.3	0.0
10	36.2	0.0	36.1	0.0
20	34.3	0.0	34.2	0.0
	NiTi (A) R→P		NiTi (B) R→P	
$\dot{T}$ /	T_R' /	σ /	T_R' /	σ /
deg·min^{-1}	°C			
0.1	37.7	0.0	37.5	0.0
1	38.0	0.0	37.6	0.0
10	37.9	0.0	37.7	0.0
20	38.2	0.0	38.2	0.0

In Figs 1–4, the values of In <*m.p.*>, Pb <*m.p.*>, and <T_R> and <T_R'> from specimen A are plotted *vs.* $\dot{T}$. Open symbols refer to uncalibrated DSC and full symbols to calibrated DSC. The least square regression lines for uncalibrated DSC are also given. The dashed line in Figs 1–2 represents the expected *m.p.*

Discussion

Tables 1 and 2 show, at all the investigated $\dot{T}$, a very good reproducibility of all the calibration standards melting points. The same applies both to the values of T_R and T_R'.

With uncalibrated DSC, as shown in Figs 1–4 (open symbols), In <*m.p.*>, Pb <*m.p.*>, <T_R> and <T_R'> verify well the linear dependence upon $\dot{T}$, as expected from Eq. (3). The calculated values of τ (Table 3) are in good agreement with literature results obtained on a similar equipment [6, 7].

Table 3 $\langle m.p.\rangle_{extr}$ of In and Pb, $\langle T_R\rangle_{extr}$ and $\langle T_R'\rangle_{extr}$ of NiTi specimens (A and B) for $\dot{T} \rightarrow 0$ with their standard deviation (σ), the slope coefficient (τ) and the correlation factor (R), as calculated by least square regression on the data in Table 1 (uncalibrated DSC)

	$\langle m.p.\rangle_{extr}$/ °C	σ / °C	τ / min	σ / min	R
In	151.1	0.0	0.093	0.004	0.997
Pb	318.2	0.0	0.098	0.004	0.997
	$\langle T_R\rangle_{extr}$/ °C	σ / °C	τ / min	σ / min	R
NiTi (A)	35.7	0.1	0.124	0.002	0.998
NiTi (B)	35.6	0.0	0.129	0.002	0.999
	$\langle T_R\rangle_{extr}$/ °C	σ / °C	τ / min	σ / min	R
NiTi (A)	35.1	0.1	0.100	0.005	0.987
NiTi (B)	34.8	0.0	0.106	0.002	0.998

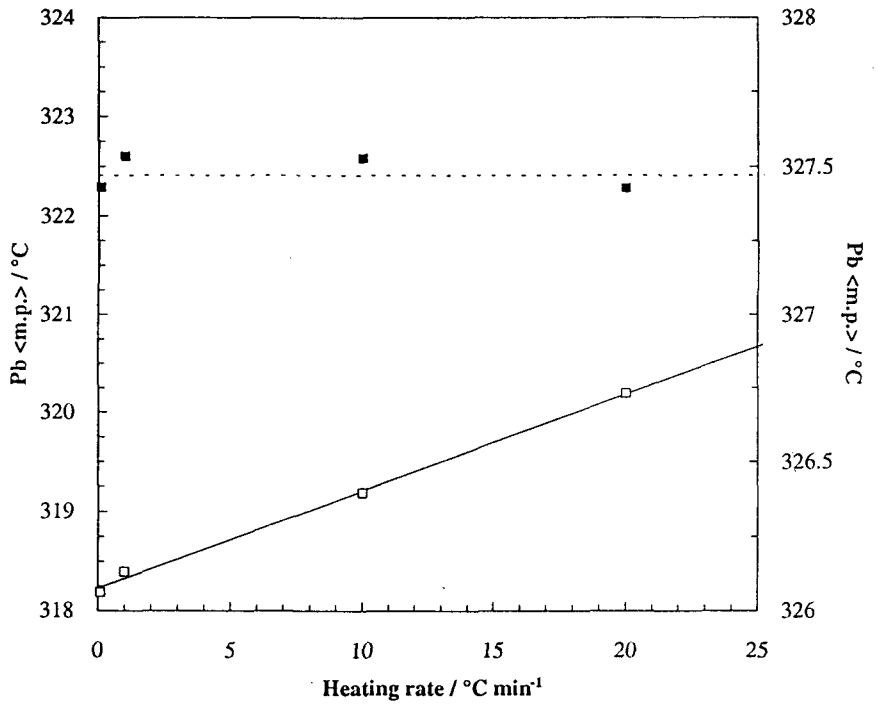

Fig. 2 Mean value of the Pb melting point ($\langle m.p.\rangle$) as a function of the heating rate, with uncalibrated DSC (left axis, open symbols) and with calibrated DSC (right axis, full symbols): the regression line (—) and the reference Pb $m.p.$ line (---) are also given

Table 4 $\langle m.p.\rangle_{extr}$ of In and Pb, $\langle T_R\rangle_{extr}$ and $\langle T_R'\rangle_{extr}$ of NiTi specimens (A and B) for $\dot{T} \rightarrow 0$ with their standard deviation (σ), the slope coefficient (τ) and the correlation factor (R), as calculated by least square regression on the data in Table 2 (calibrated DSC)

	$\langle m.p.\rangle_{extr}$/	σ /	τ /	σ /	R
	°C	°C	min	min	
In	156.6	0.0	–0.002	0.003	0.106
Pb	327.5	0.1	–0.002	0.004	0.103
	$\langle T_R\rangle_{extr}$/	σ /	τ /	σ /	R
	°C	°C	min	min	
NiTi (A)	38.5	0.1	0.211	0.010	0.995
NiTi (B)	38.5	0.1	0.220	0.008	0.998
	$\langle T_R'\rangle_{extr}$/	σ /	τ /	σ /	R
	°C	°C	min	min	
NiTi (A)	37.5	0.1	0.020	0.020	0.646
NiTi (B)	37.8	0.1	0.034	0.009	0.884

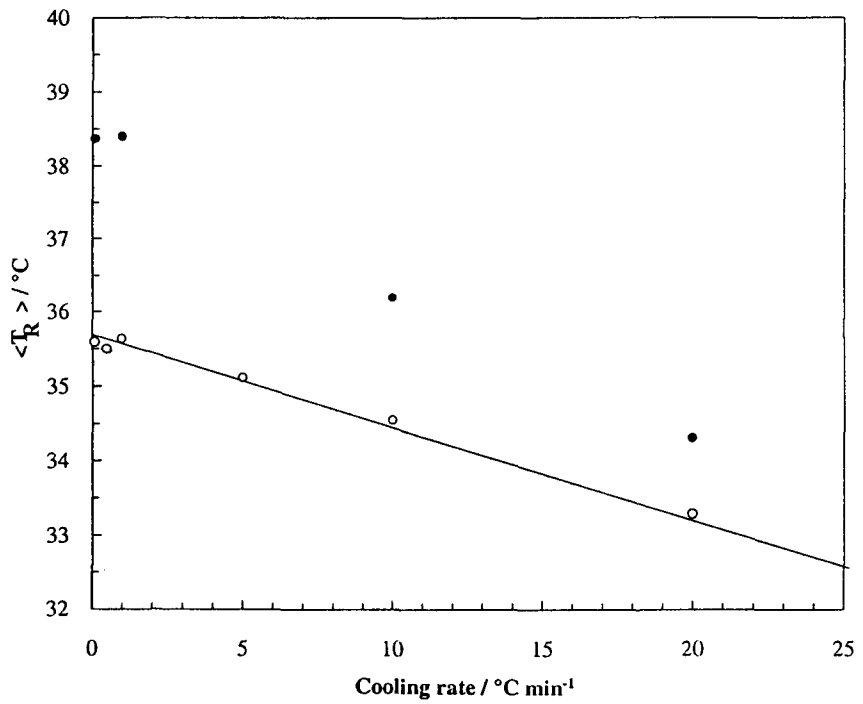

Fig. 3 Mean value of $\langle T_R\rangle$ (specimen A) as a function of the cooling rate, with uncalibrated DSC (open symbols) and with calibrated DSC (full symbols): the regression line (—) is also given

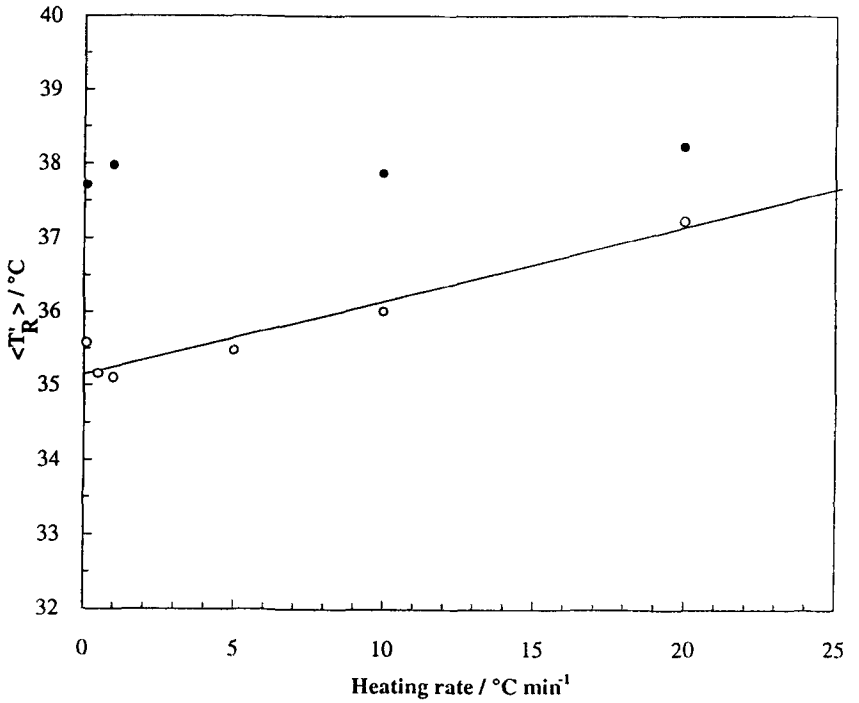

Fig. 4 Mean value of $\langle T_R' \rangle$ (specimen A) as a function of the heating rate, with uncalibrated DSC (open symbols) and with calibrated DSC (full symbols): the regression line (—) is also given

With calibrated DSC, the measurements carried out on heating have shown that In $\langle m.p. \rangle$ and Pb $\langle m.p. \rangle$ are both constant as a function of $\dot{T}$ (Figs 1 and 2, full symbols). The same applies to $\langle T_R' \rangle$ (Fig. 4, full symbols). However, on cooling, $\langle T_R \rangle$ shows a linear variation with $\dot{T}$ (Fig. 3, full symbols), even more pronounced than before calibration. The corresponding calculated value of τ (Table 4) is nearly two times the value obtained with uncalibrated DSC.

The results in Table 4 can be explained from the standard calibration Eqs (1–4). The standard calibrated temperature scale contains, through $\Delta T\,(T_{sm}, \dot{T})$, the dynamic correction $\tau_s \times \dot{T}$, evaluated *on heating*, where $\dot{T} > 0$. Unfortunately, the *same* temperature scale, that is the *same* $\Delta T\,(T_{sm}, \dot{T})$ is used *on cooling*, where $\dot{T} < 0$: in this case $\Delta T_{dyn}\,(\dot{T})$ is taken into account with the wrong sign and, therefore, a $2 \times \tau$-dependence is still expected after standard calibration. This explains clearly the nearly doubled τ-dependence of $\langle T_R \rangle$ upon $\dot{T}$ after calibration in Tables 3 and 4.

It should also be pointed out that in the standard temperature calibration, the static and the dynamic correction factors are taken into account together,

through $\Delta T(T_{sm}, \dot{T})$. Hence, intrinsically, it is not possible to correct the temperature scale on cooling, via software or hardware, because τ is not known a priori.

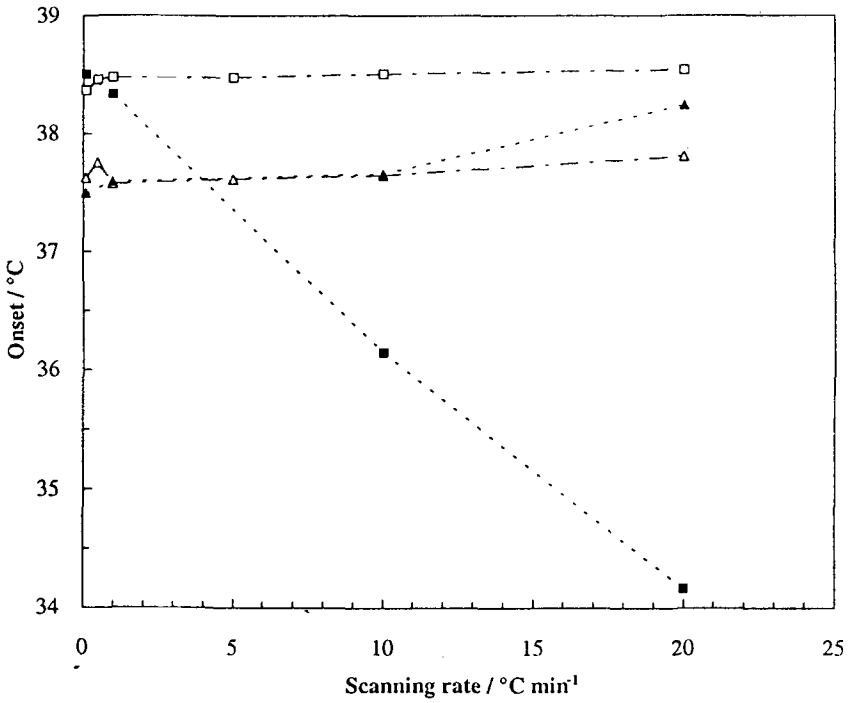

Fig. 5 $<T_R>$ (square) and $<T_R'>$ (triangle) as a function of the scanning rate (specimen B): full symbols are values obtained with the 'standard' temperature calibration; open symbols are values obtained with the uncalibrated DSC, corrected with the procedure here suggested

In order to obtain precise measurement of transformation temperatures by DSC, we suggest following the recommendation given in [7] to calculate the static temperature scale of the DSC, and performing a series of thermal runs, at different $\dot{T}$, in order to evaluate the value of τ for the specific specimen under study. This takes into account the correct dynamical error ΔT_{dyn}. Figure 5 shows the $<T_R>$ and $<T_R'>$ from specimen B as a function of $\dot{T}$, obtained with the standard calibration (full symbols) and with the protocol here suggested (open symbols). Figure 5 shows clearly the equivalence of the two procedures on heating and the discrepancy on cooling.

Conclusions

The standard DSC temperature calibration has been critically discussed in relation to the study of *TMT* in shape memory alloys. Experimental results show that, with the standard temperature calibration, the *TMT* transformation temperatures on cooling still depend upon the scanning rate, i.e. the instrument remains dynamically uncalibrated. These results are explained on the basis of the standard temperature calibration equations. A method is suggested in order to deal with this problem, based on the separate evaluation of both the static and dynamic parameters involved, through measurements performed at different scanning rates.

* * *

The work has been supported by the Project P.F.MSTA of the National Research Council (Progetto Finalizzato Materiali Speciali per Tecnologie Avanzate del Consiglio Nazionale delle Ricerche). One of the authors (G. A.) acknowledges the support of the Italian Board of Education and Research (MURST).

References

1 M. Hill and P. Nicholas, Metals and Materials, November (1989) 639.
2 'Thermal Analysis-Techniques and Applications', E. L. Charsley and B. Warrington Eds., The Royal Society of Chemistry, 1992.
3 'Differential Scanning Calorimetry', J. L. McNaughton and C. T. Mortimer, The Perkin-Elmer Corporation, Norwalk, Connecticut 06856 USA, L-604.
4 S. C. Mraw, Rev. Sc. Instrum., 53 (1982) 228.
5 ASTM E 967-83, 1984 ASTM Annual Book of Standards.
6 G. W. Höhne and E. Glöggler, Thermochim. Acta, 151 (1989) 295.
7 G. W. Höhne, H. K. Cammenga, W. Eysel *et al.*, Thermochim. Acta, 160 (1990) 1.
8 C. H. Ling and R. Kaplow, Met. Trans. A, 11A (1980) 77.
9 C. M. Wayman, Proc. Int. Symp. on Shape Memory Alloys, Eds. C. Youyi, T. Hsu and T. Ko, China Acad. Pub., 1986, p. 59.
10 S. Miyazaki, Y. Igo and K. Otsuka, Acta Metall., 34 (1986) 2045.
11 M. B. Salamon, M. E. Meichle and C. M. Wayman, Phys. Rev. B, 31 (1985) 7306.

Zusammenfassung — Außergewöhnliche mechanische Eigenschaften (z.B. Form-Memoryeffekte und Superelastizität) von Formmemory-Legierungen (SMA) beruhen auf einer thermoelastischen martensitischen Umwandlung (TMT), bei der es sich um eine athermische, nichtdiffusive Feststoff-Feststoff-Phasenumwandlung erster Ordnung handelt.
DSC wird oft als praktische Methode zur Untersuchung der thermischen Eigenschaften von SMAs benutzt. Die übliche Anwendung der für eine präzise Gerätefunktion erforderlichen Standardtemperaturkalibration wird hier in Bezugnahme sowohl auf die direkte exotherme Umwandlung beim Abkühlen als auch auf die umgekehrte endotherme Umwandlung beim Erhitzen von NiTi SMA diskutiert. Die DSC-Ergebnisse zeigen, daß das Gerät durch diese Standardtemperaturkalibration zwar für das Erhitzen, nicht aber für das Abkühlen kalibriert ist. Es wird eine allgemeine Methode zur Überwindung dieses Problemes entwickelt und in Bezug zum dynamischen Charakter der DSC gesetzt.